

# Least-Squares Based Iterative Multipath Super-Resolution Technique

Wooseok Nam, *Member, IEEE*, Seung-Hyun Kong\*, *Member, IEEE*  
 Dept. of Aerospace Engineering, KAIST,  
 Daejeon, Republic of Korea  
 E-mail: nam.wooseok@gmail.com, skong@kaist.ac.kr

## Abstract

In this paper, we study the problem of multipath channel estimation for direct sequence spread spectrum signals. To resolve multipath components arriving within a short interval, we propose a new algorithm called the least-squares based iterative multipath super-resolution (LIMS). Compared to conventional super-resolution techniques, such as the multiple signal classification (MUSIC) and the estimation of signal parameters via rotation invariance techniques (ESPRIT), our algorithm has several appealing features. In particular, even in critical situations where the conventional super-resolution techniques are not very powerful due to limited data or the correlation between path coefficients, the LIMS algorithm can produce successful results. In addition, due to its iterative nature, the LIMS algorithm is suitable for recursive multipath tracking, whereas the conventional super-resolution techniques may not be. Through numerical simulations, we show that the LIMS algorithm can resolve the first arrival path among closely arriving independently faded multipaths with a much lower mean square error than can conventional early-late discriminator based techniques.

## Index Terms

Multipath channel, super-resolution, pseudo-noise code, early-late discriminator, least-squares, maximum likelihood

## I. INTRODUCTION

A pseudo-noise (PN) code sequence, which is a deterministic but noise-like sequence generated by a linear feedback shift register, is widely used in the areas of radar and sonar signal processing, ranging and positioning, and digital communication, since it is convenient to estimate the code phase of the received signal using its peaky auto-correlation function (ACF). When the PN code sequence is launched to a channel and received by a remote terminal, the cross-correlation of the received signal and a receiver replica of the PN code sequence yields a sharp peak at the lag of the propagation delay caused by the channel. This delay is related to the physical separation between the transmitter and the receiver, and thus gives important information for source localization or target detection. However, in many practical situations, the propagation medium suffers from multiple echoes with short delays due to scattering objects around the receiver. In such a case, we are frequently interested in estimating the delays of those echoes and, especially, the first arrival path, since it is the most likely to be the line-of-sight path, which contains the information of the true distance between the transmitter and the receiver.

In the multipath channel, the conventional PN code phase estimation method using the ACF, which finds the peak of the correlator output, would probably give an incorrect estimate of the first arrival path delay unless the first arrival path is the most dominant path. This is because the ACF for the first arrival path is buried under the sum of other overlapping ACFs of echoes, and thus the lag of the largest magnitude correlator output is often different from the first arrival path delay. We can work around this problem to some extent by finding multiple local extrema of the correlator output and selecting the one with the smallest lag as the estimate of the first arrival path [1]. However, the time resolution of this

\*Corresponding author.

method is limited to the chip duration of the PN code sequence, which is not sufficient in some narrow band applications.

In order to improve resolution of the conventional ACF based code phase estimation, *super-resolution* techniques can be taken into account. The super-resolution techniques, such as the multiple signal classification (MUSIC) [2] and the estimation of signal parameters via rotation invariance techniques (ESPRIT) [3], were originally proposed for direction finding of multiple targets with passive sensor arrays, and first applied to the channel multipath resolution in [4]. In [4] and [5], the super-resolution techniques were applied directly to the received signal samples without cross-correlation. In particular, in [5], it was shown that the super-resolution techniques can be applied to received signals sampled at a considerably lower rate than the chip rate of the PN code sequence when the signals have a finite rate of innovation (FRI). On the other hand, in [6], [7], super-resolution techniques for the correlator output signal were introduced. These techniques can significantly improve the resolution of multipath delays, compared to conventional techniques, but have some major drawbacks that render them impractical. First, since the super-resolution techniques are based on the subspace decomposition of the signal correlation matrix, the signal components contributed by different channel paths should occupy distinct dimensions of the subspace in order to be distinguishable. For this, each distinct path should be far enough apart from the others, and the attenuation of each path should be varying randomly and not be perfectly correlated with the others during an observation interval. These conditions are not satisfied when the paths are quite narrowly spaced, the channel is slowly varying, or the observation interval is not long enough. In addition, it is not so reasonable to assume that only the channel attenuations are randomly varying while the path delays are fixed. As a result, additional techniques, such as frequency smoothing [6], [7], are required at the transmitter to make the assumption valid. As a second drawback, most super-resolution techniques are batch algorithms that compute a set of estimates from a large number of stationary observations. Although the technique for FRI signals [5] can work with a very small number of observations, it has very low noise immunity and also needs a large number of observations to achieve robustness against noise. The radio ranging application, however, often requires tracking of the signal as well. That is, a new observation, which can be non-stationary, is periodically given, and a new set of estimates should be immediately computed from the new observation and the previous set of estimates in a recursive manner [8], [9]. Thus, the super-resolution techniques are not adequate for applications where tracking is a concern.

In this paper, we consider a least-squares (LS) approach to resolve the short-delay multipath components with a correlator output signal. When the noise is Gaussian distributed, our approach includes the maximum likelihood (ML) approach, which is optimal in performance. The LS and ML approaches for the channel multipath resolution were presented directly and indirectly in earlier studies [10], [11], [12], but they have not gathered much interest since the highly nonlinear nature in the parameters to be estimated renders the use of these approaches computationally intensive. In [10] and [11], faster algorithms for solving a nonlinear LS problem were derived by exploiting the linear predictability of sinusoidal signals, but they are not applicable to our case. In our work, we propose an iterative algorithm to solve the LS multipath resolution problem, which we will call the *least-squares based iterative multipath super-resolution* (LIMS) algorithm. Thanks to its iterative and recursive mode of operation, it is appropriate for multipath tracking with sequential observations of the received signal. Moreover, we show that the tracking of a PN code phase using the early-late (EL) discriminator [8], [9], [13] is a special case of our algorithm. Through numerical simulations, we show that our scheme asymptotically achieves the optimal performance given by the Cramer-Rao bound (CRB) at high carrier-to-noise density ratio. In addition, we show that our algorithm outperforms the EL discriminator based technique in the presence of severe multipaths and noise.

This paper is organized as follows. In Section II, we introduce the signal model and the LS formulation for the multipath resolution. In Section III, we present the LIMS algorithm as a technique to solve the LS multipath resolution problem, and discuss the application of the LIMS algorithm for multipath tracking. The complexity of the LIMS algorithm and its relationship with the conventional EL discriminator based technique are also discussed in Section III. Results of numerical simulation in various channel models

and a comparison with the conventional method are given in Section IV, and Section V concludes the paper.

We will use the following notation throughout this paper. Vectors or matrices are denoted by boldface symbols. The  $p$ -th element of a vector and the  $(p, q)$ -th element of a matrix are denoted by  $[\cdot]_p$  and  $[\cdot]_{p,q}$ , respectively. The superscripts  $T$  and  $H$  denote the transpose and conjugate transpose, respectively. The Euclidean norm of a vector is denoted by  $\|\cdot\|$ , and the infinity norm of a vector, i.e., the largest absolute value of elements, is denoted by  $\|\cdot\|_\infty$ . The fields of real and complex numbers are indicated by  $\mathbb{R}$  and  $\mathbb{C}$ , respectively, and the  $N \times N$  identity matrix is denoted by  $\mathbf{I}_N$ . The statistical expectation is denoted by  $E\{\cdot\}$  and the real part of a complex value is denoted by  $\Re\{\cdot\}$ . Finally,  $O(\cdot)$  is the big O notation.

## II. SYSTEM MODEL

Consider a multipath channel between a transmitter and a receiver with an impulse response

$$h(t) = \sum_{k=0}^{K-1} \gamma_k \delta(t - \tau_k), \quad 0 \leq t < T_i, \quad (1)$$

where  $K$  is the number of paths,  $\{\gamma_0, \dots, \gamma_{K-1}\}$  are the unknown complex channel coefficients for each path,  $\{\tau_0, \dots, \tau_{K-1}\}$  are the unknown arrival time delays for each path,  $\delta(t)$  is the Dirac delta function, and  $T_i$  ( $\gg \max\{\tau_0, \dots, \tau_{K-1}\}$ ) is a time interval of interest. We assume that the delays  $\{\tau_0, \dots, \tau_{K-1}\}$  are distinct and  $\tau_0 < \tau_1 < \dots < \tau_{K-1}$ , without loss of generality. Thus, the delay of the first arrival path is  $\tau_0$ . The transmitter launches a continuous time PN code sequence  $s(t)$  with a chip duration  $T_c$  to the channel (1), and the baseband received signal at the receiver is written as

$$\begin{aligned} \eta(t) &= h(t) * s(t) + v(t) \\ &= \sum_{k=0}^{K-1} \gamma_k s(t - \tau_k) + v(t), \quad 0 \leq t < T_i, \end{aligned} \quad (2)$$

where  $v(t)$  is a circularly symmetric, zero-mean, complex Gaussian noise process with auto-correlation  $N_0 \delta(\zeta)$ . For the first process at the receiver, the cross-correlation of  $\eta(t)$  with  $s(t)$  is taken over the time interval  $T_i$ , and the correlator output is uniformly sampled at  $N$  lags  $\{0, T_s, \dots, (N-1)T_s\}$  to yield

$$y_n = \sum_{k=0}^{K-1} \gamma_k R(nT_s - \tau_k) + w_n, \quad n = 0, \dots, N-1, \quad (3)$$

where  $R(\zeta)$  is the auto-correlation function (ACF) of the PN code sequence given by

$$R(\zeta) = \frac{1}{T_i} \int_0^{T_i} s(t) s^*(t - \zeta) dt, \quad (4)$$

and  $w_n$  is the filtered noise process  $w(\zeta)$  sampled at  $\zeta = nT_s$ , where

$$w(\zeta) = \frac{1}{T_i} \int_0^{T_i} v(t) s^*(t - \zeta) dt. \quad (5)$$

For a binary phase shift keying (BPSK) modulated PN code sequence with a sufficiently large integration time  $T_i \gg T_c$ , the ACF (4) is ideally given by

$$R(\zeta) = \begin{cases} \frac{\zeta}{T_c} + 1, & -T_c < \zeta \leq 0, \\ -\frac{\zeta}{T_c} + 1, & 0 < \zeta \leq T_c, \\ 0, & \text{otherwise.} \end{cases} \quad (6)$$

For notational simplicity in the subsequent expressions, we denote  $\mathbf{y} = [y_0, \dots, y_{N-1}]^T$ ,  $\mathbf{c}_{\text{CH}} = [\gamma_0, \dots, \gamma_{K-1}]^T$ ,  $\mathbf{t}_{\text{CH}} = [\tau_0, \dots, \tau_{K-1}]^T$ , and  $\mathbf{w} = [w_0, \dots, w_{N-1}]^T$ . Then, from (5), the covariance matrix of the noise vector,  $E\{\mathbf{w}\mathbf{w}^H\}$ , is given by  $\frac{N_0}{T_s}\mathbf{C}$ , where  $\mathbf{C}$  has elements

$$[\mathbf{C}]_{p,q} = \frac{T_s}{N_0} E\{w_{p-1}w_{q-1}^*\} = R((p-q)T_s), \quad 1 \leq p, q \leq N. \quad (7)$$

From the above signal model, the LS estimation of the channel coefficients and the path delays is formulated as

$$\{\hat{\mathbf{c}}, \hat{\mathbf{t}}\} = \arg \min_{\mathbf{c}, \mathbf{t}} \|\mathbf{G}\mathbf{y} - \mathbf{G}\mathbf{A}(\mathbf{t})\mathbf{c}\|^2 \quad (8a)$$

$$= \arg \min_{\mathbf{c}, \mathbf{t}} \|\mathbf{G}\mathbf{y} - \mathbf{G}(\mathbf{B}(\mathbf{c}, \mathbf{t})\mathbf{t} + \mathbf{b}(\mathbf{c}, \mathbf{t}))\|^2, \quad (8b)$$

where  $\mathbf{c} = [c_0, \dots, c_{M-1}]^T \in \mathbb{C}^{M \times 1}$  and  $\mathbf{t} = [t_0, \dots, t_{M-1}]^T \in \mathbb{R}^{M \times 1}$  are the vectors of channel coefficients and path delays to be estimated, respectively, and  $M$  is the assumed number of multipaths for the estimation. Since the true number of multipaths,  $K$ , is generally unknown, we assume that  $M$  can be different from  $K$ . Note that there are two equivalent LS formulations (8a) and (8b), and the related parameters are defined as

$$[\mathbf{A}(\mathbf{t})]_{n+1, m+1} = R(nT_s - t_m), \quad (9a)$$

$$[\mathbf{B}(\mathbf{c}, \mathbf{t})]_{n+1, m+1} = \begin{cases} -\frac{c_m}{T_c}, & \frac{t_m - T_c}{T_s} < n \leq \frac{t_m}{T_s}, \\ \frac{c_m}{T_c}, & \frac{t_m}{T_s} < n \leq \frac{t_m + T_c}{T_s}, \\ 0, & \text{otherwise,} \end{cases} \quad (9b)$$

$$\mathbf{b}(\mathbf{c}, \mathbf{t}) = \sum_{m=0}^{M-1} \mathbf{b}(c_m, t_m), \quad (9c)$$

$$[\mathbf{b}(c_m, t_m)]_{n+1} = \begin{cases} c_m \cdot \left(1 + \frac{nT_s}{T_c}\right), & \frac{t_m - T_c}{T_s} < n \leq \frac{t_m}{T_s}, \\ c_m \cdot \left(1 - \frac{nT_s}{T_c}\right), & \frac{t_m}{T_s} < n \leq \frac{t_m + T_c}{T_s}, \\ 0, & \text{otherwise,} \end{cases} \quad (9d)$$

$$n = 0, \dots, N-1, \quad m = 0, \dots, M-1,$$

and  $\mathbf{G} \in \mathbb{C}^{N \times N}$  is a proper nonsingular weighting matrix. For the least-squares estimation (8) to be feasible, we assume that  $N \geq 2M$ , and  $\mathbf{A}(\mathbf{t})$  and  $\mathbf{B}(\mathbf{c}, \mathbf{t})$  have full column rank. The first assumption can be reasonable by taking a sufficient number of samples, and so is the second assumption when the delays  $\{t_0, \dots, t_{M-1}\}$  are distinct and sufficiently spaced by a small fraction of  $T_c$  [14, 2.4.7].

*Remark 1:* The signal model (3) is restricted to using the triangular shaped ACF (6) for simplicity, but it can be extended to general ACFs through a proper linearization around the sampling points. That is, for a general ACF  $R(\zeta)$ , (9b) and (9c) can be replaced by

$$[\mathbf{B}(\mathbf{c}, \mathbf{t})]_{n+1, m+1} = c_m \cdot \frac{dR(nT_s - t_m)}{dt_m}, \quad (10)$$

$$[\mathbf{b}(\mathbf{c}, \mathbf{t})]_{n+1} = \sum_{m=0}^{M-1} c_m \cdot \left( R(nT_s - t_m) - \frac{dR(nT_s - t_m)}{dt_m} t_m \right). \quad (11)$$

In addition, though we assume the uniform sampling with a sampling period  $T_s$  in (3), all the arguments in this paper can be immediately extended to non-uniform sampling.

*Remark 2:* If we let  $\mathbf{G} = \mathbf{C}^{-\frac{1}{2}}$ , the weighting matrix  $\mathbf{G}$  whitens the noise and thus the LS formulation (8) becomes the maximum likelihood (ML) formulation. In Section IV, we investigate the performance with and without noise whitening by letting  $\mathbf{G} = \mathbf{C}^{-\frac{1}{2}}$  and  $\mathbf{G} = \mathbf{I}_N$ , respectively.

### III. SOLVING THE LEAST-SQUARES MULTIPATH RESOLUTION PROBLEM

From the LS formulation (8), we can observe that it is linear in  $\mathbf{c}$  given  $\mathbf{t}$  but nonlinear in  $\mathbf{t}$  due to the dependency of  $\mathbf{B}(\mathbf{c}, \mathbf{t})$  and  $\mathbf{b}(\mathbf{c}, \mathbf{t})$  on  $\mathbf{t}$ . Thus, to find the solution to the LS problem, a computationally expensive multidimensional search seems to be inevitable. However, there exists a useful workaround to avoid an exhaustive search: the *gradient descent algorithm* [15]. The gradient descent algorithm can efficiently find the local minimum of the LS problem in an iterative manner, by stepping from the current guess of the LS solution to the direction that decreases the LS weight in (8) at every iteration. In the following subsection, we propose a gradient descent algorithm for the LS multipath resolution problem, which will be denoted by the least-squares based iterative multipath super-resolution (LIMS) algorithm.

#### A. Least-squares based iterative multipath super-resolution algorithm

For notational simplicity, let  $\tilde{\mathbf{y}} \triangleq \mathbf{G}\mathbf{y}$ ,  $\tilde{\mathbf{A}}(\mathbf{t}) = \mathbf{G}\mathbf{A}(\mathbf{t})$ ,  $\tilde{\mathbf{B}}(\mathbf{c}, \mathbf{t}) = \mathbf{G}\mathbf{B}(\mathbf{c}, \mathbf{t})$ , and  $\tilde{\mathbf{b}}(\mathbf{c}, \mathbf{t}) = \mathbf{G}\mathbf{b}(\mathbf{c}, \mathbf{t})$  in (8). The operation flow of the LIMS algorithm is described as follows. First, at the  $l$ -th iteration ( $l$  is a positive integer), the intermediate guesses of the channel coefficient and the path delay vectors,  $\mathbf{c}_{l-1}$  and  $\mathbf{t}_{l-1}$ , are given from the previous  $(l-1)$ -th iteration. Given  $\mathbf{t}_{l-1}$ , a new estimate of the channel coefficient vector,  $\mathbf{c}_l$ , is computed as

$$\mathbf{c}_l = \left( \tilde{\mathbf{A}}^H(\mathbf{t}_{l-1})\tilde{\mathbf{A}}(\mathbf{t}_{l-1}) \right)^{-1} \tilde{\mathbf{A}}^H(\mathbf{t}_{l-1})\tilde{\mathbf{y}}. \quad (12)$$

Note that the matrix inversion in (12) exists with assumptions that  $\mathbf{G}$  is nonsingular and  $\mathbf{A}(\mathbf{t})$  has full column rank. The new estimate  $\mathbf{c}_l$  (12) minimizes the LS weight in (8a) for a given  $\mathbf{t}_{l-1}$ , but it requires a matrix inversion that can sometimes be troublesome in terms of complexity or numerical stability issues. Thus, as an alternative, a refinement by the gradient descent algorithm can be used as

$$\mathbf{c}_l = \mathbf{c}_{l-1} + \alpha \cdot \tilde{\mathbf{A}}^H(\mathbf{t}_{l-1}) \left( \tilde{\mathbf{y}} - \tilde{\mathbf{A}}(\mathbf{t}_{l-1})\mathbf{c}_{l-1} \right), \quad (13)$$

where  $\alpha$  is a properly chosen step size. The refinement  $\mathbf{c}_l$  (13) does not have complexity or stability problems like (12), but may converge more slowly than (12).

For the second step, a refinement  $\mathbf{t}_l$  is computed from  $\mathbf{t}_{l-1}$  and  $\mathbf{c}_l$  using the gradient descent algorithm, for which it is required to find the gradient of the LS weight in (8b) with respect to  $\mathbf{t}$ . However, since the LS weight is nonlinear and non-analytic in  $\mathbf{t}$ , it is not easy to compute the exact gradient. Thus, we compute an approximate gradient on the basis of the following assumptions: For a small perturbation vector  $\mathbf{e}$ ,

$$\mathbf{B}(\mathbf{c}, \mathbf{t} + \mathbf{e}) \simeq \mathbf{B}(\mathbf{c}, \mathbf{t}), \quad (14a)$$

$$\mathbf{b}(\mathbf{c}, \mathbf{t} + \mathbf{e}) \simeq \mathbf{b}(\mathbf{c}, \mathbf{t}). \quad (14b)$$

From (9b), (9c), and (9d), the assumptions in (14) are quite reasonable for a magnitude of  $\mathbf{e}$  sufficiently small in the sense that  $\|\mathbf{e}\|_\infty \ll T_s$ . Under these assumptions, it can be assumed that  $\tilde{\mathbf{B}}(\mathbf{c}_l, \mathbf{t}_{l-1})$  and  $\tilde{\mathbf{b}}(\mathbf{c}_l, \mathbf{t}_{l-1})$  are constant in a small region around  $\mathbf{t}_{l-1}$ . As a result, the gradient descent for  $\mathbf{t}$  reduces to

$$\begin{aligned} \mathbf{t}_l &= \mathbf{t}_{l-1} + \beta \cdot \Re \left\{ \tilde{\mathbf{B}}^H(\mathbf{c}_l, \mathbf{t}_{l-1}) \left( \tilde{\mathbf{y}} - \left( \tilde{\mathbf{B}}(\mathbf{c}_l, \mathbf{t}_{l-1})\mathbf{t}_{l-1} + \tilde{\mathbf{b}}(\mathbf{c}_l, \mathbf{t}_{l-1}) \right) \right) \right\} \\ &= \mathbf{t}_{l-1} + \beta \cdot \Re \left\{ \tilde{\mathbf{B}}^H(\mathbf{c}_l, \mathbf{t}_{l-1}) \left( \tilde{\mathbf{y}} - \tilde{\mathbf{A}}(\mathbf{t}_{l-1})\mathbf{c}_l \right) \right\}, \end{aligned} \quad (15)$$

where  $\beta$  is a proper step size. The step size  $\beta$  should be small enough to satisfy the assumptions in (14), but a systematic criterion for  $\beta$  that guarantees the convergence is not easy to find.

Upon getting  $\mathbf{c}_l$  using (12) or (13), and  $\mathbf{t}_l$  using (15), the iteration index  $l$  is increased by one and the same computations are repeated for  $\mathbf{c}_{l+1}$  and  $\mathbf{t}_{l+1}$ . In this way, the iteration continues until a specific stop criterion is met. There are a number of stop criteria for this kind of iterative algorithm, e.g., reaching a fixed number of iterations, thresholding the magnitudes of changes of variables, etc., and we omit a detailed discussion of these criteria. The LIMS algorithm is summarized in Table I.

### B. Complexity issues

The major burden of the LIMS algorithm is the matrix inversion in (12), which is  $O(M^3)$  of computation per iteration. The true number of multipaths,  $K$ , could be large in practice and, hence, the assumed number of multipaths,  $M$ , should be accordingly large. However, assuming that only a few of the multipaths are dominant, we can keep  $M$  small; say,  $M < 10$ . Therefore, when  $N \gg M$ , the matrix inversion may not be too burdensome compared to the overall complexity. In addition, as noted in Section III-A, the matrix inversion can be avoided by using (13) instead, which is  $O(NM)$  of computation per iteration. The total number of iterations is another important factor for the complexity. However, as will be discussed in Section III-C, the number of iterations can be considerably smaller when the LIMS algorithm is combined with a tracking function such as the delay locked loop.

### C. Multipath tracking

In many practical realizations of radio ranging systems, a new observation of the received signal is obtained periodically. Successive observations may include different multipath channels when the channel is time varying. Under the assumption that the channels for the successive observations are not statistically independent, the time varying path delays can be efficiently tracked. One such tracking system is the delay locked loop (DLL) [8], [9]. In the conventional DLL used for PN code phase tracking, the early-late (EL) discriminator is widely used to generate an error signal from the previous estimate of the path delay and the new observation of the received signal (correlator output). The error signal is then filtered by the loop filter in the tracking loop and a refined delay estimate is computed. Now, instead of the EL discriminator, we consider using the LIMS algorithm in the tracking loop.

Suppose that the  $\nu$ -th observation of the received signal samples,  $\mathbf{y}^{(\nu)}$ , is given. Using the LIMS algorithm, estimates of the channel coefficient vector  $\hat{\mathbf{c}}^{(\nu)}$  and the path delay vector  $\hat{\mathbf{t}}^{(\nu)}$  are computed. Then, when the  $(\nu + 1)$ -th observation  $\mathbf{y}^{(\nu+1)}$  is given, the LIMS algorithm starts a new round of iterations with  $\hat{\mathbf{c}}^{(\nu)}$  and  $\hat{\mathbf{t}}^{(\nu)}$  as initial values. As long as  $\hat{\mathbf{c}}^{(\nu)}$  and  $\hat{\mathbf{t}}^{(\nu)}$  are good estimates of the channel coefficients and the path delays, and the channels for the  $\nu$ -th and the  $(\nu + 1)$ -th observations do not differ much, the new estimates  $\hat{\mathbf{c}}^{(\nu+1)}$  and  $\hat{\mathbf{t}}^{(\nu+1)}$  might be obtained in a small number of iterations.

When the channel is not time-varying but corrupted by different realizations of noise at different observations, applying the LIMS algorithm with a small number of iterations for each observation can be seen as the application of the *stochastic gradient method* for the channel estimation [15]. Thus, as the number of observations increases, the accuracy of channel estimation can improve until it reaches the steady state.

TABLE I  
SUMMARY OF THE LIMS ALGORITHM.

<i>Input</i>
$\mathbf{y} = [y_0, \dots, y_{N-1}]^T$
<i>Known parameters</i>
Weighting matrix: $\mathbf{G} \in \mathbb{C}^{N \times N}$
Step sizes: $\alpha$ and $\beta$
<i>Initial values</i>
$\mathbf{c}_0$ and $\mathbf{t}_0$
<i>Computation: <math>l = 1, 2, \dots</math></i>
$\mathbf{c}_l = \left( \tilde{\mathbf{A}}^H(\mathbf{t}_{l-1}) \tilde{\mathbf{A}}(\mathbf{t}_{l-1}) \right)^{-1} \tilde{\mathbf{A}}^H(\mathbf{t}_{l-1}) \tilde{\mathbf{y}}$
(or $\mathbf{c}_l = \mathbf{c}_{l-1} + \alpha \cdot \tilde{\mathbf{A}}^H(\mathbf{t}_{l-1}) \left( \tilde{\mathbf{y}} - \tilde{\mathbf{A}}(\mathbf{t}_{l-1}) \mathbf{c}_{l-1} \right)$ )
$\mathbf{t}_l = \mathbf{t}_{l-1} + \beta \cdot \Re \left\{ \tilde{\mathbf{B}}^H(\mathbf{c}_l, \mathbf{t}_{l-1}) \left( \tilde{\mathbf{y}} - \tilde{\mathbf{A}}(\mathbf{t}_{l-1}) \mathbf{c}_l \right) \right\}$
<i>Definitions</i>
$\mathbf{A}(\mathbf{t}), \mathbf{B}(\mathbf{c}, \mathbf{t})$ : given in (9)
$\tilde{\mathbf{y}} \triangleq \mathbf{G}\mathbf{y}, \tilde{\mathbf{A}}(\mathbf{t}) = \mathbf{G}\mathbf{A}(\mathbf{t}), \tilde{\mathbf{B}}(\mathbf{c}, \mathbf{t}) = \mathbf{G}\mathbf{B}(\mathbf{c}, \mathbf{t})$

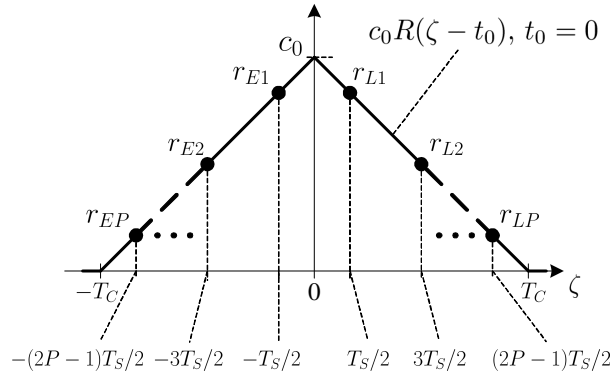


Fig. 1. Sampling  $c_0 R(\zeta - t_0)$  at  $2P$  points.

#### D. Relationship with the conventional early-late discriminator

The EL discriminator computes the difference between the powers (magnitude squares) of two samples with different lags at the correlator output. The two samples are called the early and the late samples and are separated by a constant interval. When the peak of an ACF is located in between the two samples, the difference between the two powers serves as a feedback signal that shifts the sampling points so that the peak of the ACF is at the midpoint of the sampling points. Intuitively, this operation is established on the assumptions that the channel has a single path and that the correlator output maintains the exact triangular shape of the ACF  $R(\zeta)$  (6). However, these assumptions are not valid when the channel has multiple paths and the received signal is corrupted by noise.

Basically, the EL discriminator can be thought of as a special case of the LIMS algorithm with the single path assumption, i.e.,  $M = 1$ , and two samples, i.e.,  $N = 2$ . To illustrate this relationship, let us first consider  $2P$  sampling points at  $\zeta = \frac{(2p+1)T_s}{2}$ ,  $p = -P, \dots, P-1$ , where  $P = \left\lfloor \frac{T_c}{T_s} + \frac{1}{2} \right\rfloor$ . Then, at the sampling points, the sampled values of the correlator output are denoted by  $y_{E(-p)}$  for  $p < 0$  and  $y_{L(p+1)}$  for  $p \geq 0$ . Likewise, the sampled values of the scaled ACF,  $c_0 R(\zeta - t_0)$ , are denoted by  $r_{E(-p)}$  for  $p < 0$  and  $r_{L(p+1)}$  for  $p \geq 0$ , as shown in Fig. 1. Now, we temporarily let  $T_s = T_c$ , and thus  $P = 1$  and the number of total samples is  $N = 2P = 2$ . Assuming  $-\frac{T_c}{2} < t_0 \leq \frac{T_c}{2}$  and the number of paths  $M = 1$ , the LS weight is given by

$$\left\| \begin{bmatrix} y_{E1} \\ y_{L1} \end{bmatrix} - \begin{bmatrix} r_{E1} \\ r_{L1} \end{bmatrix} \right\|^2 \quad (16a)$$

$$= \left\| \begin{bmatrix} y_{E1} \\ y_{L1} \end{bmatrix} - c_0 \begin{bmatrix} 0.5 - t_0 \\ 0.5 + t_0 \end{bmatrix} \right\|^2 \quad (16b)$$

$$= \left\| \begin{bmatrix} y_{E1} \\ y_{L1} \end{bmatrix} - c_0 \begin{bmatrix} -1 \\ 1 \end{bmatrix} t_0 - c_0 \begin{bmatrix} 0.5 \\ 0.5 \end{bmatrix} \right\|^2. \quad (16c)$$

Note that, since the two samples are one chip apart, the noise levels for the two samples are independent according to (7). Hence, by Remark 2, (16) is the ML weight as well. From (9), parameter vectors for the LS weight (16) are defined as

$$\mathbf{A}(t_0) = \begin{bmatrix} 0.5 - t_0 \\ 0.5 + t_0 \end{bmatrix}, \quad (17a)$$

$$\mathbf{B}(c_0, t_0) = c_0 \begin{bmatrix} -1 \\ 1 \end{bmatrix}, \quad (17b)$$

$$\mathbf{b}(c_0, t_0) = c_0 \begin{bmatrix} 0.5 \\ 0.5 \end{bmatrix}. \quad (17c)$$

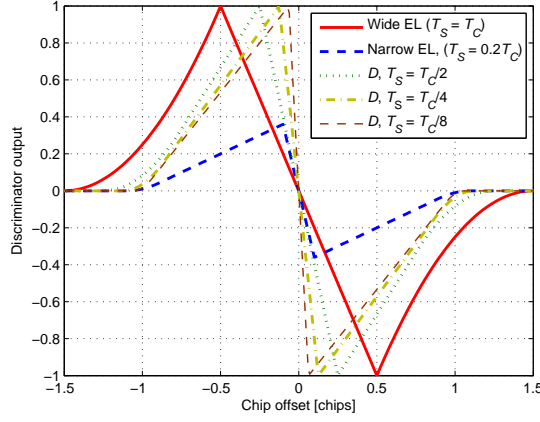


Fig. 2. Discriminator responses.

Applying the LIMS algorithm to the LS weight (16) with the initial value  $t_{0,0} = 0$ , the first iteration gives

$$c_{0,1} = (\mathbf{A}^H(t_{0,0})\mathbf{A}(t_{0,0}))^{-1} \mathbf{A}^H(t_{0,0}) \begin{bmatrix} y_{E1} \\ y_{L1} \end{bmatrix} = y_{E1} + y_{L1} \quad (18)$$

by (12), and  $t_{0,1} = t_{0,0} - \beta D$  by (15), where

$$\begin{aligned} D &= -\Re \left\{ \mathbf{B}^H(c_{0,1}, t_{0,0}) \left( \begin{bmatrix} y_{E1} \\ y_{L1} \end{bmatrix} - c_{0,1} \mathbf{A}(t_{0,0}) \right) \right\} \\ &= -\Re \{ (y_{E1} + y_{L1})^* (y_{E1} - y_{L1}) \} \\ &= |y_{E1}|^2 - |y_{L1}|^2. \end{aligned} \quad (19)$$

As expected,  $D$  (19), the approximate gradient with respect to  $t_0$ , is the same as the EL discriminator.

Similarly, for  $T_s < T_c$ , we can derive

$$D = -\Re \{ \mathbf{B}^H(c_{0,1}, 0) \mathbf{C}^{-1} (\mathbf{y} - c_{0,1} \mathbf{A}(0)) \}, \quad (20)$$

where  $\mathbf{y} = [y_{EP}, \dots, y_{E1}, y_{L1}, \dots, y_{LP}]^T$ ,

$$c_{0,1} = (\mathbf{A}^H(0) \mathbf{C}^{-1} \mathbf{A}(0))^{-1} \mathbf{A}^H(0) \mathbf{C}^{-1} \mathbf{y}, \quad (21)$$

and  $\mathbf{A}(0)$  and  $\mathbf{B}(c_{0,1}, 0)$  are defined similarly to (17), by letting  $M = 1$  in (9). Note that, in (20) and (21), noise whitening is applied. Then, (20) can be regarded as a generalized  $2P$ -point discriminator as an extension of the conventional 2-point discriminator like the EL discriminator. The quantity  $D$  as a function of the code phase offset for different values of  $T_s$  is evaluated and plotted in Fig. 2. The discriminator responses of the EL discriminators with sample spacing  $T_c$  (wide discriminator) and  $0.2T_c$  (narrow discriminator) are also plotted in Fig. 2 for comparison. In the figure, it is observed that, as  $T_s$  decreases, the discriminator curve gets steeper around the zero offset, which implies stronger resistance against perturbation after the DLL is locked at the peak of the ACF [13].

#### IV. NUMERICAL RESULTS

This section presents simulation results to demonstrate the performance of the LIMS algorithm. For comparison, the conventional EL discriminators for PN code phase tracking with wide ( $T_c$ ) and narrow ( $0.2T_c$ ) spacings are also considered. In particular, performance is evaluated with the estimation accuracy of the delay of the first arrival path and, as the performance measure, the mean square error (MSE) of the delay estimate is used. For all simulations, the results are obtained by averaging over  $10^4$  trials with



independent realizations of noise and channel impulse response. As for the PN code sequence, we use the global positioning system (GPS) coarse-acquisition (C/A) code sequence [16], which has 1023 chips per period with a 1.023MHz chip rate; one chip occupies  $T_c = 1/(1.023 \times 10^6)$  seconds. The received signal is generated by superimposing the attenuated, phase rotated, and delayed replicas of the C/A code sequence according to the multipath channel realization, and adding white Gaussian noise with the power spectral density  $N_0$ . The received carrier power is defined as  $C = E \{|h(t) * s(t)|^2\}$  in (2), where the expectation is over the channel realizations. The carrier power  $C$  varies resulting in a carrier to noise density ratio ( $C/N_0$ ) between 20dBHz and 60dBHz. At the receiver, the integration time of the correlator,  $T_i$ , is set to be 10ms, which corresponds to 10 periods of the GPS C/A code sequence.

For all simulations, it is assumed that a window of the correlator output signal of  $3T_c$  width is available for the EL discriminator and the LIMS algorithm. The center of the window is defined as the zero lag, i.e.,  $\zeta = 0$ . It is also assumed that the coarse acquisition of the PN code phase is perfect regardless of  $C/N_0$  so that the true first arrival path is placed at a random lag uniformly distributed over  $[-0.5T_c, 0.5T_c]$ . Note that, since the size of the observation is too small to compute the sample correlation matrix of the received signal, conventional super-resolution techniques like MUSIC and ESPRIT cannot be applied to the considered simulation environment.

### A. Simulation system

For the simulation of the LIMS algorithm, the sampling period  $T_s = 0.1T_c$  is used. As described in Section III-A, equation (12) is used for the channel coefficient update and, for ease of implementation, the signed gradient descent algorithm is used in place of (15) for the delay update. That is,

$$\mathbf{t}_l = \mathbf{t}_{l-1} + \beta \cdot \text{sgn} \left[ \Re \left\{ \tilde{\mathbf{B}}^H(\mathbf{c}_l, \mathbf{t}_{l-1}) \left( \tilde{\mathbf{y}} - \tilde{\mathbf{A}}(\mathbf{t}_{l-1})\mathbf{c}_l \right) \right\} \right], \quad (22)$$

where  $\text{sgn}[\cdot]$  is the element-wise sign function. For the step size  $\beta$  in (22), we use  $\beta = T_s/64$ . To start the iteration, the initial value  $\mathbf{t}_0 = [t_{0,0}, \dots, t_{M-1,0}]^T$  is given such that  $t_{0,0} = -0.5T_c$ ,  $t_{M-1,0} = 0.5T_c$ , and  $t_{m,0}$ ,  $0 < m < M - 1$  evenly divide the interval  $(-0.5T_c, 0.5T_c)$ . With this initial value, the final estimates of the channel coefficient vector  $\hat{\mathbf{c}} = [\hat{c}_0, \dots, \hat{c}_{M-1}]^T$  and the delays vector  $\hat{\mathbf{t}} = [\hat{t}_0, \dots, \hat{t}_{M-1}]^T$  are obtained by  $\mathbf{c}_{500}$  and  $\mathbf{t}_{500}$ , respectively.

Upon completion of the estimation process, a simple path validation process follows to reduce the probability of false alarm; an estimated path is valid if the estimated power ( $|\hat{c}_m|^2$ ) of the path is larger than 1% of the total estimated power ( $\sum_{m=0}^{M-1} |\hat{c}_m|^2$ ). The path with the smallest delay among the valid paths is chosen for the first arrival path.

Finally, in the simulations of the LIMS algorithm, two different cases, without noise whitening, i.e.,  $\mathbf{G} = \mathbf{I}_M$ , and with noise whitening, i.e.,  $\mathbf{G} = \mathbf{C}^{-1/2}$ , are included for comparison.

### B. Two-path non-fading channel

The first test channel considered for simulation is a two-path non-fading channel with  $\mathbf{c}_{\text{CH}} = \left[ \frac{1}{\sqrt{2}}, \frac{1}{\sqrt{2}} \right]^T$  and  $\mathbf{t}_{\text{CH}} = \left[ 0, \frac{T_c}{2} \right]^T$ . The performance results in terms of the MSE with respect to  $C/N_0$  are shown in Fig. 3(a). As a benchmark, the CRB, which is derived in Appendix, is also plotted in the same figure. With this channel, the correlator output has a flat top when there is no noise. As a result, the conventional EL discriminator, which assumes a single path and the triangular ACF, cannot perform well with the channel. On the other hand, the LIMS algorithm can handle the two paths simultaneously and outperforms the EL discriminator. It is also observed that the LIMS algorithm with noise whitening consistently performs better than that without noise whitening. In particular, at high  $C/N_0$ 's, the LIMS algorithm with noise whitening asymptotically achieves the CRB.

In Fig. 3(b), learning curves of the LIMS algorithm with noise whitening for the first arrival path delay are depicted for 50 independent trials at  $C/N_0 = 30\text{dBHz}$ . Observe that, even with a very large initial deviation, the algorithm successfully converges to the vicinity of the true first arrival path delay within 300 iterations.

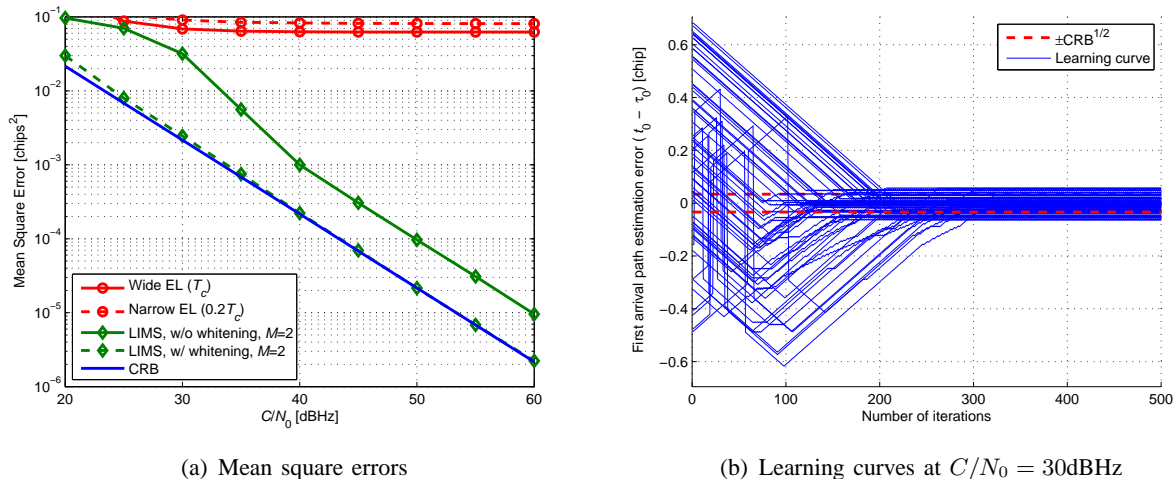


Fig. 3. Mean square errors and learning curves of the first arrival path delay estimation:  $\mathbf{c}_{\text{CH}} = [1/\sqrt{2}, 1/\sqrt{2}]^T$  and  $\mathbf{t}_{\text{CH}} = [0, T_c/2]^T$ .

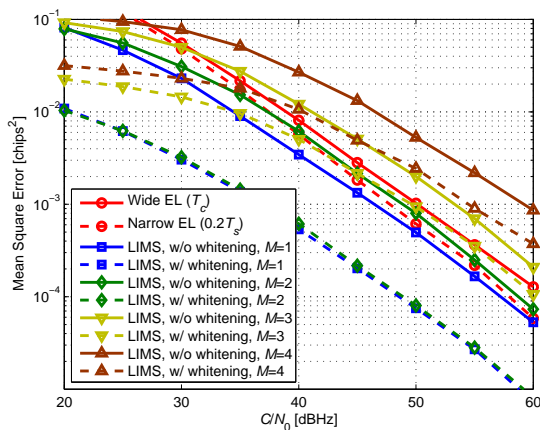


Fig. 4. Mean square errors of the first arrival path delay estimation: Single-path fading channel.

### C. Single-path fading channel

For the second simulation, a channel with only one path is considered, where the channel coefficient  $\gamma_0$  is a zero-mean circular symmetric complex Gaussian random variable with  $E\{|\gamma_0|^2\} = 1$ . The MSE performances of the EL discriminators and the LIMS algorithms with different settings for this channel are plotted in Fig. 4. As shown in the figure, the EL discriminators, especially the one with narrow spacing, perform very well for the channel. This is because the assumption that the correlator output has a triangular shape, on which the EL discriminator is based, is valid for this case. Among all performance curves plotted in Fig. 4, the best is achieved by the LIMS algorithm with  $M = 1$  and noise whitening. Compared to the performance of the EL discriminators, the best performance is an order of magnitude superior. In terms of the generalized discriminator presented in Section III-D, this performance improvement arises from the fact that the LIMS algorithm can make use of a larger number of received signal samples and thus has a steeper discriminator response. Finally, in Fig. 4, note that the LIMS algorithm with  $M = 2$  and noise whitening has a performance comparable to that with  $M = 1$  and noise whitening even though the number of assumed paths is not the same as the true value.

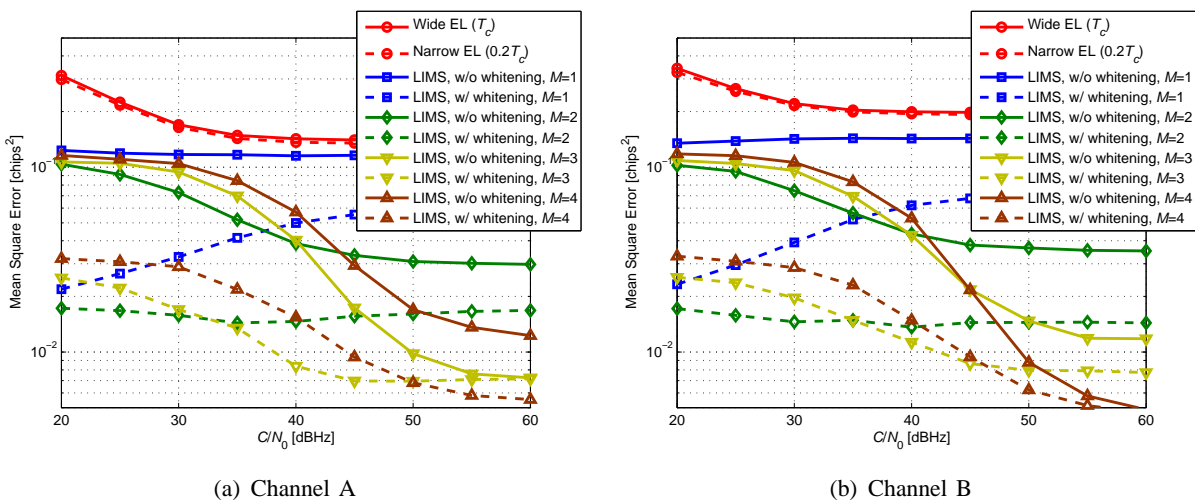


Fig. 5. Mean square errors of the first arrival path delay estimation: Multipath fading channels without band limitation.

#### D. Multipath fading channels

The third test channel models considered for simulation are the multipath fading channels. Two multipath fading channel models, which are denoted by channels A and B, respectively, are considered. Channels A and B have three and four paths, respectively, and the power-delay profiles are given in Table II. Note that, for both channels, the average power of the first arrival path is 7dB lower than that of the strongest path. With the given power-delay profiles, the channel coefficients are generated independently as zero-mean circular symmetric complex Gaussian random variables with corresponding variances for each trial. The MSE performances of the EL discriminators and the LIMS algorithms with different settings are plotted in Figs. 5(a) and 5(b) for channels A and B, respectively. In Figs. 5(a) and 5(b), it is observed that the EL discriminators yield very poor performances. This is because the EL discriminator tends to keep track of the largest magnitude point at the correlator output, which would be located mostly near the strongest path and hardly near the first arrival path. Due to the same reason, the performance of the LIMS algorithm with  $M = 1$  is also bounded. However, the LIMS algorithms with  $M \geq 2$  show much better performances since they can track multiple paths simultaneously, and one of the tracked paths is possibly close to the true first arrival path.

The effect of limited bandwidth on the performance should also be investigated. In practice, the received signal is bandlimited to the pre-correlation bandwidth by a band pass filter before the cross-correlation with the PN code sequence replica, and thus the ACF may not have as sharp a triangular shape as (6) has [17, 4.2]. This causes a mismatch between the assumed signal model and the true signal, and can entail some performance loss. For the simulation, an ideal band pass filter with a rectangular frequency response centered at the carrier frequency of the signal is assumed. Figs. 6(a) and 6(a) show the results obtained for channels A and B, respectively, when an 8MHz pre-correlation bandwidth is applied. By comparing Figs. 5 and 6, it is found that there is no significant loss when using an 8MHz pre-correlation

TABLE II  
PARAMETERS OF THE THREE- AND FOUR-PATH FADING CHANNELS.

Path	Channel A		Channel B	
	Relative power (dB)	Delay ( $T_c$ )	Relative power (dB)	Delay ( $T_c$ )
1	-7.0	0	-7.0	0
2	0	0.3	-7.0	0.2
3	-2.2	0.5	0	0.4
4	-	-	-2.2	0.6

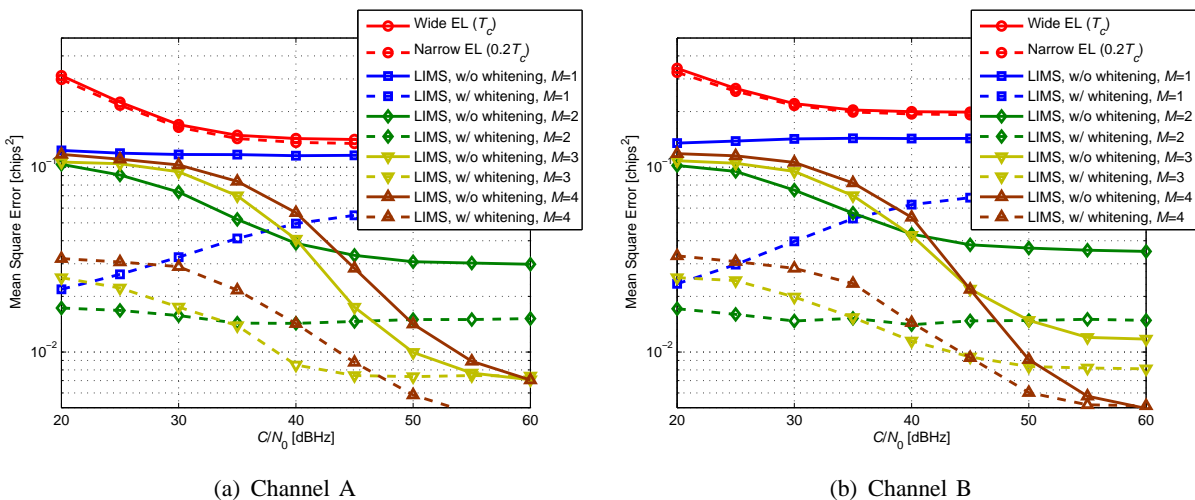


Fig. 6. Mean square errors of the first arrival path delay estimation: Multipath fading channels with 8MHz pre-correlation bandwidth.

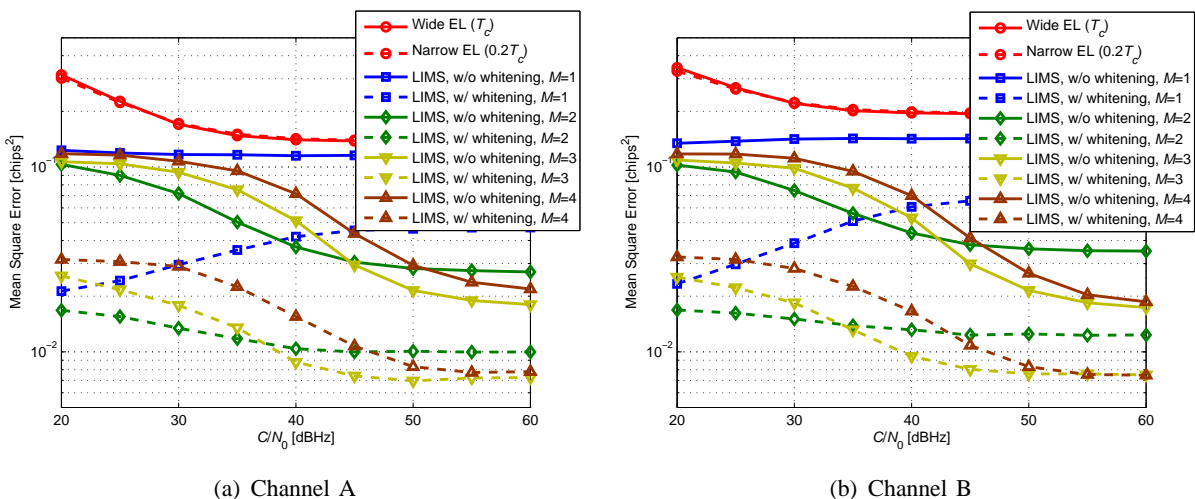


Fig. 7. Mean square errors of the first arrival path delay estimation: Multipath fading channels with 2MHz pre-correlation bandwidth.

bandwidth. The results with a 2MHz pre-correlation bandwidth are also shown in Figs. 7(a) and 7(b). There is apparent loss in this case, especially for the LIMS algorithms with  $M = 3$  and  $M = 4$  at high  $C/N_0$ 's. However, the performance loss is still not significant, and, therefore, one can conclude that the LIMS algorithm is quite robust to the band limitation.

## V. CONCLUSION

In this paper, the multipath channel estimation problem for direct sequence spread spectrum signals was investigated. A new technique based on the least-squares criterion, denoted as the least-squares based iterative multipath super-resolution (LIMS) algorithm, was proposed for the resolution of short delay multipaths. Unlike conventional super-resolution techniques such as MUSIC and ESPRIT, the LIMS algorithm does not rely on subspace decomposition, and, therefore, has practical advantages. In particular, the LIMS algorithm can work with a short observation of the received signal regardless of the correlation between path coefficients. In addition, due to its iterative operation, the LIMS algorithm is suitable for recursive multipath tracking. We also presented a view of the LIMS algorithm as a generalization of the conventional EL discriminator for PN code phase tracking. Through numerical simulations, it was shown that the performance of the LIMS algorithm is superior to that of the EL discriminator in estimating the

delay of the first arrival path. As a result, the LIMS algorithm can be a useful technique for applications such as radio ranging, global navigation satellite systems (GNSSs), radio propagation analysis, and time synchronization and multipath tracking in wireless communication systems.

## APPENDIX

### THE CRAMER-RAO BOUND FOR THE FIRST ARRIVAL PATH DELAY ESTIMATION

From the signal model (3), the inverse Fisher information matrix [18, B.3.3] for the estimation of the channel coefficients and the path delays is computed as

$$\mathbf{F}^{-1} = \frac{T_i}{2N_0} (\Re \{ \mathbf{D}^H \mathbf{C}^{-1} \mathbf{D} \})^{-1}, \quad (23)$$

where  $\mathbf{D} \in \mathbb{C}^{N \times 2K}$  is a concatenated matrix defined as

$$\mathbf{D} = [\mathbf{A}(\mathbf{t}_{\text{CH}}) \quad \mathbf{B}(\mathbf{c}_{\text{CH}}, \mathbf{t}_{\text{CH}})], \quad (24)$$

and  $\mathbf{A}(\cdot)$  and  $\mathbf{B}(\cdot, \cdot)$  are defined in (9). The mean square error (MSE) of each parameter estimation is lower bounded by the corresponding diagonal element of the inverse Fisher information matrix. Thus, the MSE of the first arrival path delay estimation is lower bounded by the  $(K + 1)$ -th diagonal element of the inverse Fisher information matrix (23).

## REFERENCES

- [1] T. S. Rappaport, "Characterization of UHF multipath radio channels in factory buildings," *IEEE Trans. Antennas Propagat.*, vol. 37, No. 8, pp. 1058–1069, Aug. 1989.
- [2] R. O. Schmidt, "Multiple emitter location and signal parameter estimation," *IEEE Trans. Antennas Propagat.*, vol. AP-34, pp. 276–280, Mar. 1986.
- [3] R. Roy and T. Kailath, "ESPIRIT estimation of signal parameters via rotational invariance techniques," *IEEE Trans. Acoust., Speech, Signal Processing*, vol. 37, No. 7, pp. 984–995, July 1989.
- [4] A. M. Bruckstein, T.-J. Shan, and T. Kailath, "The resolution of overlapping echos," *IEEE Trans. Acoust., Speech, Signal Processing*, vol. ASSP-33, No. 6, pp. 1357–1367, Dec. 1985.
- [5] J. Kusuma, I. Maravić, and M. Vetterli, "Sampling with finite innovation rate: Channel and timing estimation in UWB and GPS," in *Proc. ICC*, May 2003.
- [6] T. Manabe and H. Takai, "Superresolution of multipath delay profiles measured by PN correlation method," *IEEE Trans. Antennas Propagat.*, vol. 40, No. 5, pp. 500–509, May. 1992.
- [7] F. Bouchereau, D. Brady, and C. Lanzl, "Multipath delay estimation using a superresolution PN-correlation method," *IEEE Trans. on Signal Processing*, vol. 49, No. 5, pp. 938–949, May. 2001.
- [8] J. W. Betz and K. R. Kolodziejki, "Generalized theory of code tracking with an early-late discriminator. Part I: Lower bound and coherent processing," *IEEE Trans. Aerospace and Electronic Systems*, vol. 45, No. 4, pp. 1538–1550, Oct. 2009.
- [9] J. W. Betz and K. R. Kolodziejki, "Generalized theory of code tracking with an early-late discriminator. Part II: Noncoherent processing and numerical results," *IEEE Trans. Aerospace and Electronic Systems*, vol. 45, No. 4, pp. 1551–1564, Oct. 2009.
- [10] R. Kumaresan and A. K. Shaw, "High resolution bearing estimation without eigendecomposition," in *Proc. IEEE Int. Conf. Acoust., Speech, Signal Processing*, Tampa, FL, pp. 576–579, Mar. 1985.
- [11] Y. Bresler and A. Macovski, "Exact maximum likelihood parameter estimation of superimposed exponential signals in noise," *IEEE Trans. Acoust., Speech, Signal Processing*, vol. ASSP-34, pp. 1081–1089, Oct. 1986.
- [12] P. Stoica and A. Nehorai, "MUSIC, maximum likelihood, and Cramer-Rao bound," *IEEE Trans. Acoust., Speech, Signal Processing*, vol. 37, No. 5, pp. 720–741, May. 1989.
- [13] M. Irsigler and B. Eissfeller, "Comparison of multipath mitigation techniques with consideration of future signal structures," in *Proc. ION GPS/GNSS*, Portland, OR, Sep. 2003.
- [14] D. Muñoz, F. Bouchereau, C. Vargas, and R. E.-Caldera, *Position Location Techniques and Applications*, Academic Press, 2009.
- [15] S. Haykin, *Adaptive Filter Theory*, fourth edition, Prentice Hall, 2002.
- [16] Pratap Misra and Per Enge, *Global Positioning System: Signals, Measurements, and Performance*, second edition, Ganga-Jamuna Press, 2001.
- [17] K. Yu, I. Sharp, and Y. J. Guo, *Ground-Based Wireless Positioning*, Wiley, 2009.
- [18] P. Stoica and R. Moses, *Introduction to Spectral Analysis*, Englewood Cliffs, 1997.